


LETTER

Open Access



Green synthesis of silver nanoparticles and its antibacterial activity using fungus *Talaromyces purpureogenus* isolated from *Taxus baccata* Linn.

Ankush Sharma^{1*} , Anand Sagar¹, Jagriti Rana¹ and Reena Rani²

Abstract

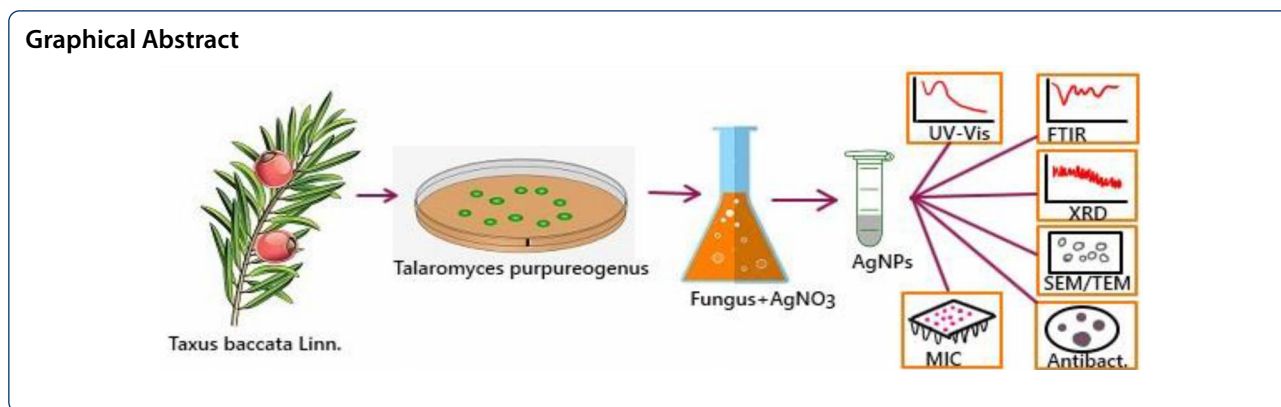
The present study is focused on the synthesis of silver nanoparticles (AgNPs) utilizing endophytic fungus *Talaromyces purpureogenus*, isolated from *Taxus baccata* Linn. Extracellular extract of *Talaromyces purpureogenus* has shown occurrence of secondary metabolites viz. terpenoids and phenols. Gas chromatography-mass spectroscopy analysis showed the presence of 16 compounds. Techniques like Ultraviolet-visible spectroscopy, Fourier transform infrared spectroscopy, dynamic light scattering, field emission gun scanning electron microscopy, high-resolution transmission electron microscopy, energy-dispersive X-ray spectroscopy and X-ray diffraction were employed to characterize the synthesized AgNPs. UV-Vis spectroscopy showed sharp peaks at 380–470 nm which indicates the presence of metallic silver. FTIR analysis showed the presence of various functional groups like phenols, hydroxyl groups, and primary amines. In DLS, Z-average size and Pdl of synthesized AgNPs were 240.2 r.nm and 0.720 respectively, with zeta potential – 19.6 mV. In FEG-SEM and HRTEM the spherical AgNPs showed diameter in the range of 30–60 nm. In EDS analysis the weight percent of Ag is 67.26% and atomic percent is 43.13%. From XRD analysis the size of AgNPs was found to be 49.3 nm with face-centered cubic crystalline nature of fungal synthesized AgNPs. These nanoparticles have shown significant antibacterial activity against tested strains viz. *Listeria monocytogenes* (13 ± 0.29 mm), *Escherichia coli* (17 ± 0.14 mm), *Shigella dysenteriae* (18 ± 0.21 mm) and *Salmonella typhi* (14 ± 0.13 mm). These synthesized AgNPs have shown effective free radical scavenging activity against 2,2'-diphenyl-1-picrylhydrazyl. The present study showed that the endophytic fungus *Talaromyces purpureogenus* can be used as a prominent source to synthesize AgNPs by using biological, ecofriendly, and in a non-toxic way accompanied by antibacterial and antioxidant properties which further can reduce the harvesting pressure faced by *Taxus baccata*.

Keywords: *Talaromyces purpureogenus*, *Taxus baccata* Linn., AgNPs, DLS, XRD, HRTEM-EDS, Antibacterial and antioxidant activity

*Correspondence: theankushsharma@gmail.com

¹ Department of Biosciences, Himachal Pradesh University, Summerhill, Shimla 171005, Himachal Pradesh, India

Full list of author information is available at the end of the article



Introduction

Gymnosperms are majorly exploited for their wood quality, resins, gums, and medicinal values [1]. *Taxus baccata* Linn. a gymnosperm found at a height of 2300–2800 m in the western and eastern Himalayas, has innumerable medicinal utilities such as those used in kidney disease, Alzheimer [2], bronchitis, asthma, and as an aphrodisiac [3]. Apart from these uses bark is used as salted tea by the local community [4] paste of the bark is used to cure headaches and as a plaster to repair the fractured bones [5]. The plant is supposed to be a good source of anti-cancerous drugs Taxol or Paclitaxel [6, 7]. However, the utilitarian values of this plant are causing its degradation in several ways. Lack of good harvesting techniques and statutory procedures, the leaves and bark are harvested callously leading to the injudicious exploitation of the plants. Also, the excessive stress on this plant for its resources for commercial uses and habitat disturbances are resulting in its disappearance at a rapid rate [8–10]. *Taxus baccata* is a splendid host of many types of microorganisms such as endophytic bacteria (*Burkholderia* and *Enterobacter*) [11], endophytic fungi (*Aspergillus*, *Fusarium*, *Penicillium*, *Trichoderma*, etc. [12, 13] and mycorrhizae [12, 14]. Endophytic fungi reside in the plant's internal tissues without causing any visible harm to them. These fungi have been reported to synthesize a variety of chemical compounds called secondary metabolites, reported to possess antibacterial, antifungal, anti-cancerous, antioxidant, and various other important activities [15–17].

The tissue extracts of *Taxus baccata* are the source of many medicines. A further advanced step has been employed where nano-sized particles coated with tissue extracts of *Taxus baccata* work more precisely than the ordinary processes [18, 19]. However, this dependency on the plant can be minimized by the use of fungi for the production of anti-cancerous materials encapsulated on nanoparticles [20–22]. Nanobiotechnology has emerged as a promising technology to develop new therapeutically

active nanomaterials; nanoparticles are one of them [23]. Nanoparticles exhibit special optical, electronic, and magnetic properties [24]. Nanoparticles having exceptionally tiny size result in strong adherence to the target sites and are not easily washed away in the system, thus increasing their residence time on the targets such as cancer cells. This increase in retention time results in better drug delivery and cure to the problem [25].

Exposure of secondary metabolites reduces the metallic ions into nanosized metallic particles [26]. Among other metallic nanoparticles silver nanoparticles has been immensely worked upon due to their biocompatibility [27]. Silver nanoparticles possess variety of beneficial properties including optical, good electrical conductivity and biological properties. Applications of silver nanoparticles is increasing as antibacterial agents, sensors, food industry and as anticancerous agents. Biologically synthesized silver nanoparticles possess high solubility, stability, high yield and antimicrobial properties. The process of AgNPs synthesis is also non-toxic and cost effective [28–31]. Synthesis of many fungus-coated metallic nanoparticles has been reported [32–36]. A very important fungus *Penicillium* sp. isolated from a useful plant named *Glycosmis mauritiana*, has been reported to effectively produce AgNPs which are showing good quality antioxidant, antimicrobial, anti-inflammatory, and tyrosinase inhibitory activity [37]. Fungus *Talaromyces pupureogenus* isolated from *Pinus* sp. resulted in the formation of AgNPs with an average size of 25 nm and has shown strong antibacterial and antioxidant properties [22]. *Taxus baccata* is also considered to be a host of many fungal species [12, 38]. AgNPs of size 5–70 nm with spherical shape were obtained from fungus *Nemania* sp. isolated from *Taxus baccata*. These AgNPs have shown prominent antibacterial activity against certain harmful bacteria [38]. So, in the present study fungus, *Talaromyces pupureogenus* isolated from a gymnosperm *Taxus baccata* has been utilized for the synthesis of AgNPs and the characterization of these nanoparticles has been done

using various spectrophotometric techniques. Further, the activity of these AgNPs has been tested as antibacterial and antioxidant agents.

Experimental

Isolation and identification of endophytic fungi

Healthy tissues (leaf, stem, and roots) of *Taxus baccata* were collected from the Choordhar region of Shimla District of Himachal Pradesh, India. The tissues were sterilized in the lab by using the method of Schulz et al. [39]. The plant tissues were properly washed under running tap water. The surface sterilization was done by first immersing in 70% ethanol for 60 s, followed by sodium hypochlorite (4% of available chlorine) for 3 min and then dipped in 75% of ethanol for 30 s. For the sterilization of leaves, the method of Suryanarayan and Thennarasan [40] was followed. The leaf samples were cut into pieces of different sizes. Finally, sterilized samples were rinsed with autoclaved distilled water three times and were allowed to dry in laminar airflow. The plant samples such as root, bark, stem, and leaves were cut into small pieces and placed on the Petri plates containing potato dextrose agar (PDA, Himedia Pvt. Ltd. India). The PDA was also supplied with streptomycin (100 mg/L, Himedia Pvt. Ltd. India) to prevent endophytic bacterial growth. Petri plates were incubated at 28 ± 2 °C. These Petri plates were observed on regular basis for endophytic fungal growth. A pure culture of the endophytic fungi was obtained after continuous transfer of hyphal tips on fresh PDA plates. Morphological identification of the isolated endophytic fungi was performed at ARI Pune, India (Agharkar Research Institute). Out of 08 endophytic fungi 07 (*Aspergillus flavus*, *A. nidulans*, *A. niger*, *Penicillium viridicatum* etc.) belonged to family Aspergillaceae and one (*Talaromyces purpureogenus*) to Trichomaceae. Molecular-level identification of isolated fungi was carried by PCR using ITS4 and ITS5 primer pair. The identification was being carried out at ARI Pune, India (Agharkar Research Institute). *T. purpureogenus* formed soft and cottony ascocarps with interwoven hyphae. The fruiting body of this particular fungus were yellowish in colour. Structures like conidia, metulae and phialides were observed carefully. The phialides were supported by the metulae. Further, identification of the fungus was done when the genomic DNA was isolated in pure form from the culture. The ITS-rDNA partial gene was successfully amplified using ITS4 and ITS5. The sequencing PCR was set up with ABI-BigDye® Terminatorv 3.1 Cycle Sequencing Kit. The raw sequence obtained from ABI 3100 automated DNA sequencer was manually edited for inconsistency. The sequence data was aligned with publicly available sequences and analyzed to reach identity. All isolated endophytic fungi were screened for

antibacterial activity and *T. purpureogenus* showed significant activity against tested bacterial strains. Therefore, it was further selected for the synthesis of AgNPs.

Preparation of endophytic fungal extracts

T. purpureogenus was inoculated in potato dextrose broth (PDB) and was incubated at 28 ± 2 °C on an incubator shaker with 150 rpm for 6 days. The growth of the fungus was observed regularly. This fungal biomass was filtered with the help of Whatman filter paper no. 1. This filtered mass was washed 3 times with distilled water to remove the media. For the preparation of endophytic fungal extracts, two standard procedures [41, 42] were used. The harvested fungal mass was weighed and 20 g of it was transferred to a 500 mL Erlenmeyer flask containing 100 mL of distilled water. These flasks were incubated at 28 ± 2 °C for 24 h with the 180 rpm shaking for the extraction. At the end of this period, the cell-free filtrate was filtered using Whatman No. 1 filter paper and used in further experimental processes.

Screening for secondary metabolites

For the screening of secondary metabolites, the method of Radji et al. [43] was followed with slight modifications. Small rectangular blocks from the agar plates containing fungal mycelium were cut and inoculated into a 250 mL Erlenmeyer flask containing 100 mL of (PDB). After pouring the flasks were incubated at $25\text{--}27$ °C for 21 days with occasional shaking. After the defined period, the broth culture was filtered to separate mycelium and filtrate. The extraction was performed with majorly 05 organic solvents and after standardization ethyl acetate was preferred as extraction solvent because of better results as compared to other organic solvents. Since, ethyl acetate is less polar than alcoholic extract, it dissolves the hydrocarbon rich secondary metabolites much better than alcohols. Insights into previous works also substantiated the selection of the solvent [44, 45]. An equal volume of ethyl acetate was added to the filtrate. The solution was mixed well for 10–15 min and then kept for 5–10 min. The formation of two clear immiscible layers was observed. The upper layer of ethyl acetate was separated using a separating funnel as it contains the extracted compounds. Rotary evaporation supplemented with reduced pressure at $35\text{--}40$ °C was done to remove the solvents and resulting in a concentrated extract. Further, the extract was dissolved in DMSO and stored in the refrigerator. The qualitative screening of phytochemicals present in the fungal extract was done by following the standard procedure of Devi et al. [46].

GCMS analysis of fungal extract

Mass spectrum of compounds was done by gas chromatography-mass spectroscopy (GCMS analyser-Thermo Scientific TSQ 8000 Gas Chromatograph—Mass Spectrometer). It was paired with GC TRACE-1300 GC. The ion source was EI source programmable to 350 °C with mass range 2.1100 a.m.u and column temperature 400 °C. The column used was Rtx-5 of 30 m in length, 0.25 mm column inside diameter with 0.25 µm film coating. The sample was filtered through Whatman Filter Device (0.2 µm). Helium (99.99%) gas was used as the carrier with a flow rate of 1 mL/min in split mode. A volume of 1 µL of the fungal extract was injected into the column with 280 °C inlet temperature. The temperature of the oven was initially set at 70 °C for 2 min and then it was elevated at a rate of 7 °C/min up to 320 °C. The temperature of ion sources was maintained at 250 °C. The mass spectrum of compounds present in the fungal extract was obtained by electron ionization at 70 eV and the detector operates in scan mode 30–500 Da atomic units. The total running time was 22.77 min with 6694 scans. The obtained spectrum of the extract was compared with the database of the National Institute of Science and Technology (NIST) library [47].

Biosynthesis and characterization of AgNPs

For the synthesis of AgNPs from *Talaromyces purpureogenus*, method of Sandhu et al. [48] was opted with little modifications. An aqueous solution of silver nitrate (80 mL; 2 mM) was mixed with 20 mL of fungal extract and incubated at room temperature. Flasks were kept covered with aluminium foil to reduce the chances of photo-oxidation. Prior standardization of reaction mixture was done before proceeding towards the final process of nanoparticle synthesis. According to the standardization the time limits were finalized which were corresponding to the color change and AgNPs synthesis. The aliquots of samples were withdrawn subsequently after 12 h, 24 h, 36 h, 48 h, 72 h, and 96 h for observing the color change from transparent to dark brown.

For the determination of successful synthesis of AgNPs UV–Vis spectrophotometry (Shimadzu UV–Vis Spectrophotometer) was done by measuring the absorbance of the solution at different time intervals (1, 12, 24, 48, 72, and 96 h) at 300–700 nm. After 48–72 h of reaction, the mixture was centrifuged at 12,000 rpm for 15 min. The unbounded capping material was removed by repeated washing (4 times) with double distilled water. Thereafter, the pellet was lyophilized to get dry powder of the material. There are different types of functional groups involved in the stabilization and capping of synthesized nanoparticles which were detected by using FTIR. Characteristic peaks were recorded in 400–4000 cm⁻¹ at

resolution 4 cm⁻¹. The sample was analyzed twice. The size was analyzed with the help of Dynamic Light Scattering analysis (DLS-Malvern). Surface morphological studies were done using FEGSEM technique. However, for the elemental analysis, FEGSEM-EDS was used. For the analysis of the shape and size of synthesized nanoparticles the AgNPs powder was suspended in ethanol for High-Resolution Transmission Electron Microscopy (HRTEM) and the presence of specific metallic groups was found with the help of HRTEM-EDX (energy-dispersive X-ray spectroscopy). Finally, XRD was used for the analysis of morphology and crystalline nature of AgNPs in a wide range of Bragg angles 2θ at scanning rate 30–80 at 0.041/min with a time constant of 2 s.

Antibacterial activity

To determine the antibacterial activity of AgNPs disc diffusion method was used as described by Brumfitt et al. [49]. This method was preferred over other methods based on literature, its promising and precise results [22]. All the bacterial strains (*Listeria monocytogenes*, *Shigella dysenteriae*, *E. coli*, and *Salmonella typhi*) were cultured in 10 mL of MHB in 50 mL Erlenmeyer flask for 24 h at 37 °C. Fifty µL of the bacterial cell suspension was spread over the MHA plates. Further, discs of 6 mm diameter were prepared from Whatman filter paper-3 which was further autoclaved and sterilized. These discs were dipped in different concentrations of solution of AgNPs. For positive control discs were supplied with antibiotics (Vanomycin and Ampicillin, 0.1 mg/mL). The plates with antibiotics were used as positive control and those with DMSO were used as a negative control. These paper discs were placed on each plate which was further incubated at 37 °C for 24 h. The antibacterial activity of AgNPs was measured as a clear zone of inhibition (mm) using a vernier caliper.

The lowest concentration of an antibacterial agent to inhibit/prevent the growth of bacterial growth is called minimum inhibitory concentration (MIC). For the determination of MIC values of synthesized AgNPs microbroth dilution method of Sarkar et al. [50] was followed. Fifty µL of each sterile nutrient broth and normal saline was added to each well of the micro-titre plate. Now 50 µL of nanoparticle solution was dissolved in DMSO (25 mg/mL). This 50 µL was added to the first row of the micro-titre plate followed by serial dilution across the plate. Ten µL of each resazurin dye (indicator) and bacterial inoculums were added to each well. Plates were wrapped properly in a cling film to prevent the process of dehydration of bacteria and incubated at 37 °C for 24 h. These experiments were performed in duplicates to avoid any sort of error. A change in the color of the solution in

the well was observed. If the color changes from purple to pink or colorless it indicated that bacteria have grown in it. The lowest concentration at which no color change was observed was considered as MIC value of AgNPs.

Antioxidant assays

For the determination of antioxidant potential of *T. purpureogenus* and synthesized AgNPs two assays viz. DPPH assay and reducing power assay were performed.

DPPH (1, 1-diphenyl-2-picrylhydrazyl) free radical scavenging activity

The antioxidant activity of the synthesized silver nanoparticles was determined by DPPH (1,1-diphenyl-2-picryl-hydrazyl) free radical scavenging assay as given by Blois [51]. One mL of extract prepared in 10% DMSO of different concentrations (30 µg/mL, 60 µg/mL, 90 µg/mL, 120 µg/mL and 150 µg/mL) along with standard made up of DPPH + DMSO. One mL of 0.3 mM DPPH was added to it under dark conditions and was incubated for 30 min in dark. The absorbance was taken at 517 nm by UV–Vis spectrophotometer (UV-1800 Shimadzu). Ascorbic acid was used as reference or standard with same concentrations (30 µg/mL, 60 µg/mL, 90 µg/mL, 120 µg/mL and 150 µg/mL). The percent inhibition was calculated by the formula given below:

$$\% \text{ inhibition} = \frac{\text{Abs}_{(\text{Control})} - \text{Abs}_{(\text{sample})}}{\text{Abs}_{(\text{Control})}} \times 100$$

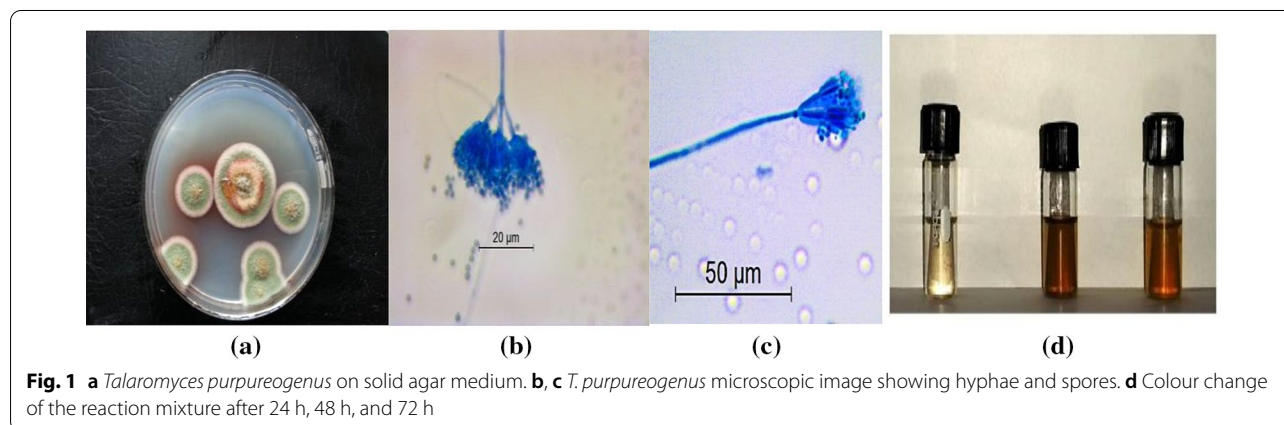
The amount of extract that quenches 50% free radicals of DPPH is called its IC₅₀ value. IC₅₀ value (µg/mL) was determined by plotting a graph of % inhibition against different concentrations of extracts.

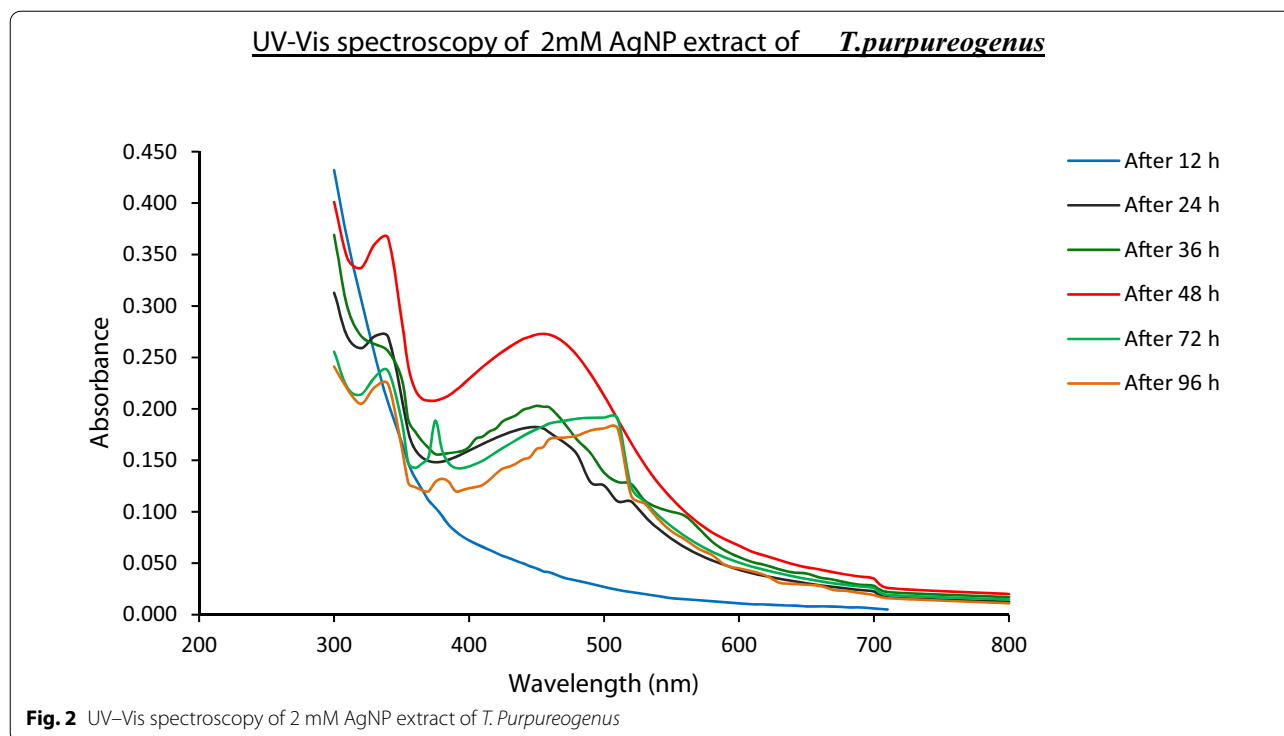
Reducing power assay

For the estimation of reductive potential of the fungal extract and AgNPs the method of Oyaizu [52] was followed. Ascorbic acid was taken as standard. One mL of distilled water was mixed with fungal extracts/AgNPs and standard (1 mg/mL). This solution was further mixed with phosphate buffer (2.5 mL, 0.2 mol/L, pH 6.6) and potassium ferricyanide (2.5 mL, 1% w/v) was added to the mixture. The solution was mixed properly and centrifuged for 10 min at 3000 rpm. Then, 2.5 mL of supernatant was mixed with 2.5 mL of distilled water and 0.5 mL of FeCl₃ (0.1% w/v). The absorbance was measured at 700 nm in UV–Vis spectrophotometer (UV-1800 Shimadzu). The experiment was performed in triplicates. The high value of the absorbance in reaction mixture indicated a greater reducing power of the fungal extract and AgNPs.

Results and discussion

Molecular identification of the fungal strain was done using ITS4 and ITS5 sequencing. The tested fungal strain showed 100% sequence similarity with *Talaromyces purpureogenus*. Sequence analysis with NCBI accession number MK108916.1, *Talaromyces purpureogenus* strain KNUPD2 resulted in the following alignment statistics. Query length—531, score—958 bits (1062), Expect—0.0, Identities—531/531 (100%), Gaps—0/531 (0%), Strand—Plus/Plus. The BLASTn and NCBI analyzed the sequence identification by homology search for the sequence closely related to the fungal species. This fungus holds the potency of secreting a variety of secondary metabolites. Secondary metabolites viz. Terpenoids and phenols have shown their presence in *Talaromyces purpureogenus* broth, however, tannins and alkaloids were found to be absent from both the broth extract and mycelial extract. These phenols possibly play a vital role in antioxidant properties of the materials. GC–MS analysis of





T. purpureogenus extract indicated the presence of 16 compounds when compared with NIST Database. Major compounds identified were Dibutyl phthalate, Phthalic acid, butyl hept-3-yl ester (57.90%), 9, 12-Octadecadienoic acid, methyl ester (29.60%), 2 amino-4-hydroxy 6-methyl pyrimidine (4.17%), and Apiole (2.31%).

The colour of the reaction mixture i.e., mycelial extract and AgNO_3 was observed at regular intervals which changed from white to orangish brown after 48 h (Fig. 1b, c). This color change can be correlated with the process of excitation of surface plasmon vibration within the biologically produced AgNPs [53]. In UV-vis spectroscopy a peak was obtained at 390–460 nm by UV-visible spectroscope (Fig. 2).

During the spectral analysis, spectroscopy was done at regular intervals predefined during standardization. Maximum absorbance was observed at 450 nm which is a characteristic surface plasmon resonance peak of mycosynthesized AgNPs [54], the results are similar to previous findings [55, 56]. The peaks obtained at 438 nm wavelength probably give nanoparticles with size a size range of 60–80 nm [57]. These results are in accordance with the previous results [19, 58–61]. FTIR (Fig. 3) showed the bands at 3428.4 cm^{-1} confirming the presence of hydroxyl group, H-bonded –OH stretch [62]. A peak at 1621.9 cm^{-1} showed the presence of amides or primary amine with N–H bend. A peak at 1383.9 cm^{-1} confirmed the presence of phenols or tertiary alcohol

–OH bend. A peak at 1076.1 cm^{-1} corresponds to –C–N primary amine stretch or cyclic ether with large rings, C–O stretch. Peaks at 1022.0 cm^{-1} correspond to aromatic C–H in-plane bend. The peak at 516.0 cm^{-1} may correspond to the presence of aryl disulfide (S–S) or Polysulfides (S–S stretch) or C–Br stretch [63]. This concludes that these functional groups are somehow involved in the stabilization of AgNPs and act as a capping agent [64]. These results were in accordance with the previous results [38, 65].

DLS (dynamic light scattering) measurement with zeta potential was used to find out the average size of AgNPs (Fig. 4). The Z-average was 240.2 nm with 0.720, PDI value (Fig. 4a). Zeta potential having either high negative value or high positive value, show a tendency to repel each other thus declining the agglomeration [65, 66]. The polydispersed nature of the nanoparticles is a result of highly negative zeta potential avoiding the formation of agglomerates leading to a concise stability. The obtained nanoparticles have zeta potential equal to -19.5 mV (Fig. 4b) attesting the repulsive nature of the silver nanoparticles leading to the stability [67, 68]. Present X-ray diffraction analysis demonstrated that the nature of synthesized AgNPs is crystalline (Fig. 5). The XRD pattern of synthesized AgNPs is shown in Fig. 5. The result of XRD analysis indicated the 2θ value of 38° , 46° , 67° and 78° correspond to 111, 200, 220, and 311 respectively to the planes of silver. The XRD results confirmed the

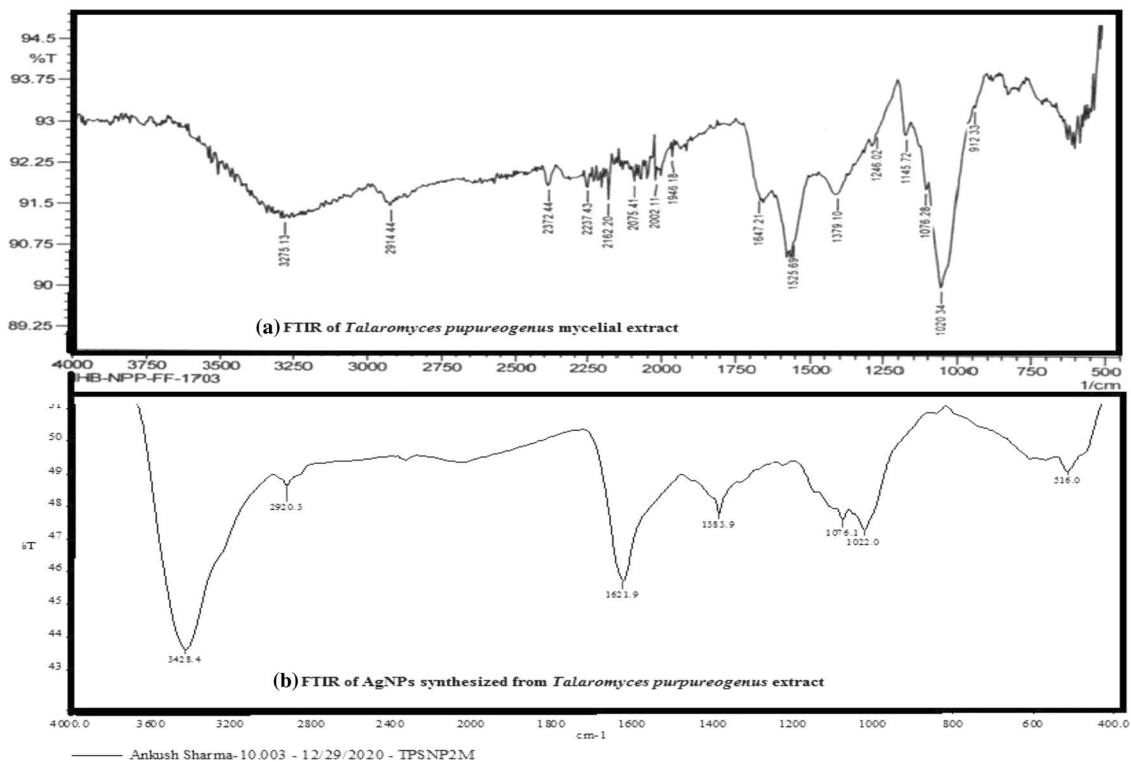


Fig. 3 FTIR showing peaks for specific functional groups, **a** fungal extract, **b** *T. purpureogenus* AgNPs

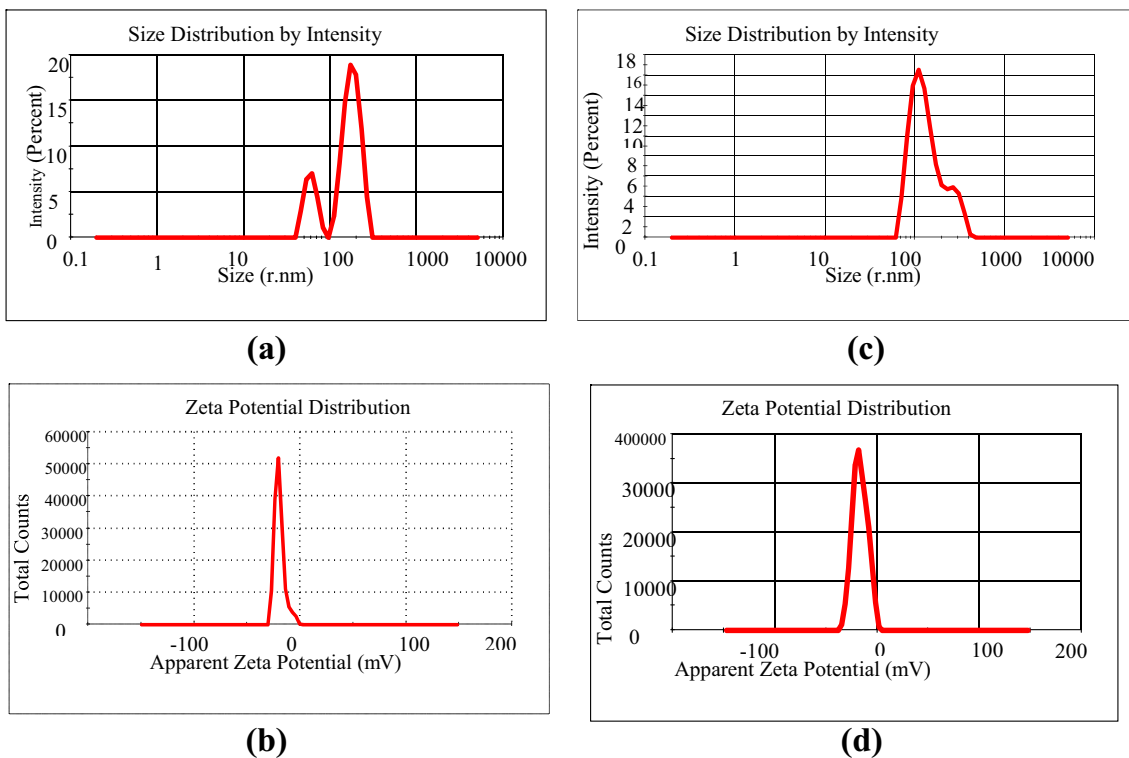


Fig. 4 DLS and Zeta Potential analysis of *T. Purpureogenus* AgNPs showing. **a** Size distribution by intensity first day. **b** Zeta Potential Distribution First day. **c** Size distribution by intensity after 60 days. **d** Zeta Potential Distribution after 60 days

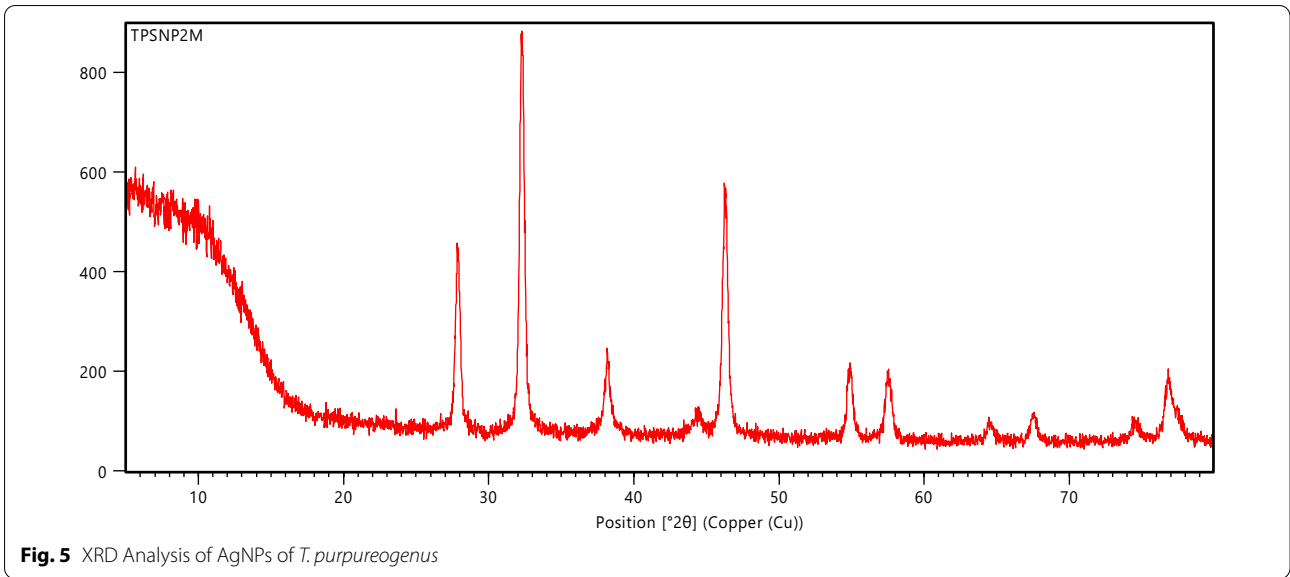


Fig. 5 XRD Analysis of AgNPs of *T. purpureogenus*

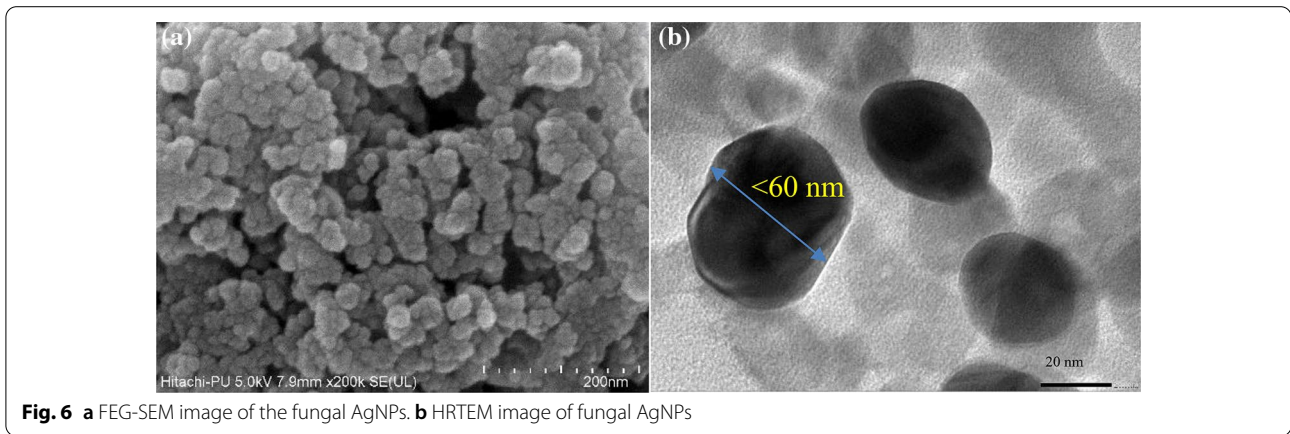


Fig. 6 **a** FEG-SEM image of the fungal AgNPs. **b** HRTEM image of fungal AgNPs

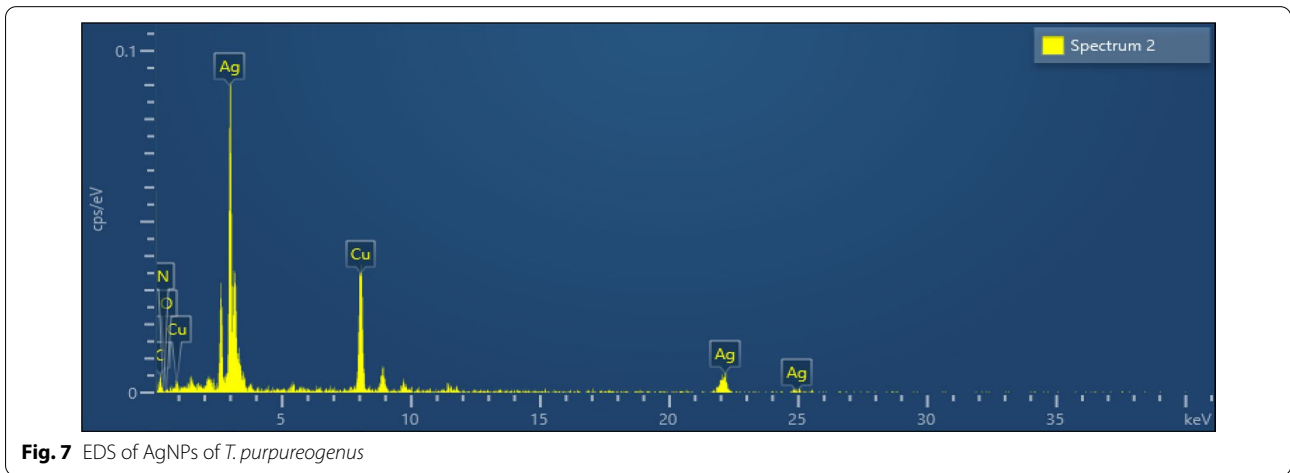


Fig. 7 EDS of AgNPs of *T. purpureogenus*

occurrence of AgNPs. These results also confirmed the nature of AgNPs as crystalline face-centered cubic which is in agreement with the database of JCPDS (now called ICDD) file no. 04-0783. These results are as per the previous XRD results of biosynthesized AgNPs [17, 49, 56, 60, 69, 70].

The morphological features of mycosynthesized AgNPs were observed in FEG-SEM (Fig. 6a) which showed a variety of shapes and sizes of AgNPs with few clump formations. AgNPs have shown cauliflower-like morphology in FEG-SEM (Fig. 6a), which are in accordance with the previous results [50]. HRTEM (Fig. 6b) results revealed that the synthesized AgNP's were round to oval/round shaped [71] and having a diameter ranging from 30 to 60 nm. The EDX analysis confirmed the presence of 0.63% of Ag atoms. The HRTEM-EDS (Fig. 7) analysis showed the weight percent of Ag 67.26% and atomic percent 43.13%. The presence of

mycosynthesized AgNPs was confirmed by the specific peak at 3.0 keV in EDS.

Peaks showing presence of carbon, oxygen and copper also appeared in EDS micrograph (Fig. 7). Generally, the samples are coated on copper-grid whose remnants may have resulted in the peak shown at 8 keV. These results were following the previous results [55, 58]. The stability of the synthesized silver nanoparticles was observed for 50–60 days by three parameters viz. UV–vis spectroscopy, DLS analysis and FTIR analysis. Here, UV–vis spectroscopy showed absorption peaks in range of 440–480 nm. Further, the Z-average size of AgNPs was 304.7 r.nm with Pdl 0.807 (Fig. 4c). The zeta potential was observed to be – 16.6 mV, still a good quality result (Fig. 4d) The specific peaks at 3317.0, 1041.0 and 1589.0 cm^{-1} were observed quite similar to the points discussed earlier (Fig. 3). This stability of nanoparticles play a vital role in antimicrobial potential.

In the present study these mycosynthesized AgNPs showed a prominent antibacterial activity (Fig. 8) against a list of bacterias viz. *E.coli*, *Shigella sp.*, *Salmonella typhi* (gram-negative), and *Listeria sp.* (gram-positive) which was similar to positive control vanomycin and ampicillin. The highest zone of inhibition was found to be in the case of *E. coli* (17.00 ± 0.14 mm), followed by *Shigella sp.* (18.00 ± 0.21 mm) and *Salmonella typhi* (14.00 ± 0.13 mm). The lowest zone of inhibition was found to be in *Listeria sp.* (13.00 ± 0.29 mm) (Table 1). These results were found to be in accordance with the previous reports [72–74]. Further, MIC analysis was opted for testing antibacterial activity against above 4 strains of bacteria. MIC of fungal extract for the different bacterial strains was 31.25 $\mu\text{g/mL}$ (*Listeria* and *Shigella*), 125 $\mu\text{g/mL}$ (*E.coli*) and 62.5 $\mu\text{g/mL}$ (*S. typhi*). MIC of mycosynthesized silver nanoparticles for different bacterial strains was 1.5625 $\mu\text{g/mL}$ (*Listeria* and *Shigella*), 0.78125 (*E. coli*) and 3.125 (*S. typhi*).

DPPH analysis (Fig. 9a) was performed for the assessment of antioxidant properties of the fungal extract and mycosynthesized AgNPs. The percent inhibition in the

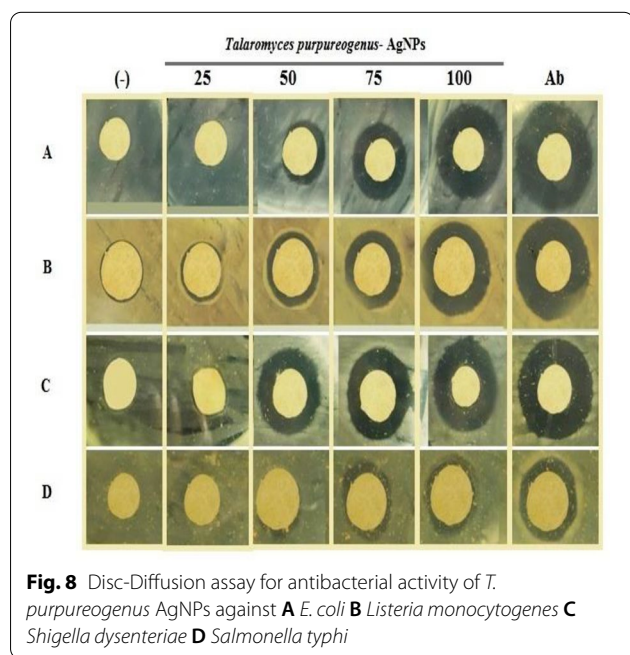
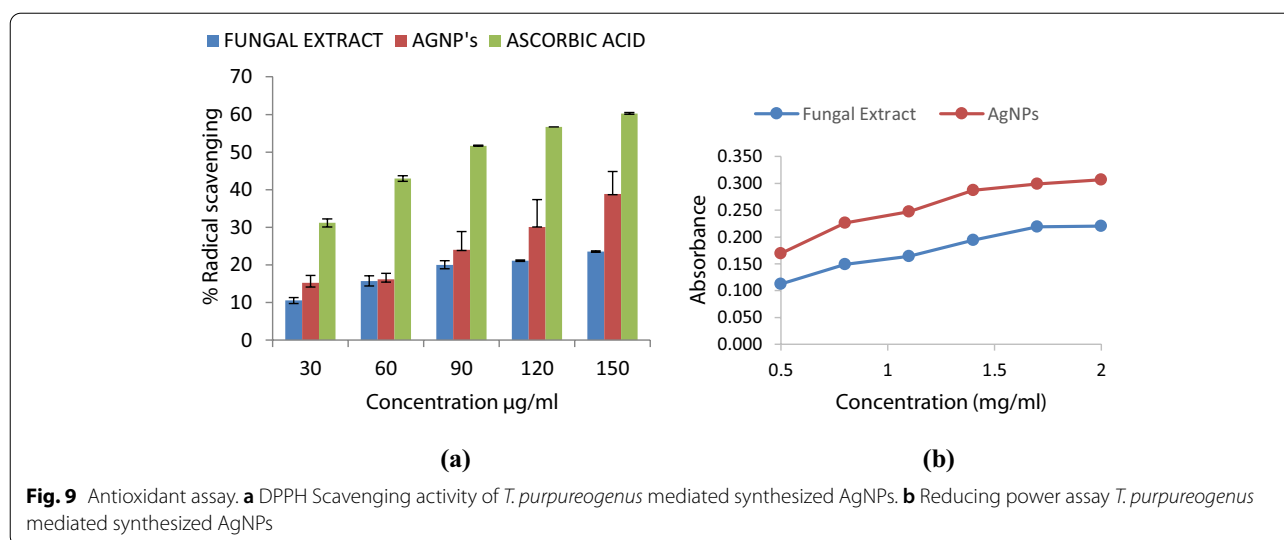


Fig. 8 Disc-Diffusion assay for antibacterial activity of *T. purpurpureogenus* AgNPs against **A** *E. coli* **B** *Listeria monocytogenes* **C** *Shigella dysenteriae* **D** *Salmonella typhi*

Table 1 Antibacterial activity of *T. purpurpureogenus* AgNPs against (1) *Listeria monocytogenes* (2) *Shigella dysenteriae* (3) *E. coli* (4) *Salmonella typhi*

Serial no.	Bacterial strain	Positive control (+) ampicillin/vanomycin (mm)	Negative control (-) DMSO (mm)	25 $\mu\text{g/mL}$ (I) (mm)	50 $\mu\text{g/mL}$ (I) (mm)	75 $\mu\text{g/mL}$ (I) (mm)	100 $\mu\text{g/mL}$ (I) (mm)
1	<i>Listeria monocytogenes</i>	18 ± 0.16	6 ± 0.17	9 ± 0.26	11 ± 0.42	12 ± 0.32	14 ± 0.29
2	<i>Shigella dysenteriae</i>	21 ± 0.19	6 ± 0.16	10 ± 0.23	15 ± 0.16	17 ± 0.23	18 ± 0.21
3	<i>E. coli</i>	26 ± 0.14	6 ± 0.16	12 ± 0.16	16 ± 0.19	19 ± 0.16	23 ± 0.14
4	<i>Salmonella typhi</i>	16 ± 0.15	6 ± 0.17	8 ± 0.14	12 ± 0.15	13 ± 0.15	15 ± 0.13



case of the fungal extract was found to be 10.554% at lower concentration and 23.571% at high concentration; similarly, the percent inhibition in the case of mycosynthesized AgNPs was found to be 15.215% at lower concentration and 32.894% at high concentration. The IC_{50} values for fungal extract and AgNPs were 393.6361 and 250.3009 $\mu\text{g}/\text{mL}$ respectively. The reducing potential was measured by change of Fe^{3+} to Fe^{2+} . The AgNPs showed high absorbance value than the fungal extract (Fig. 9b) that indicated their enormous reductive potential and ability to donate electrons for free radical stabilization. From the results, it can be assumed that the mycosynthesized AgNPs performed better as antioxidant agents when compared to the fungal extract. This effective result can be beneficial to consider them a good source of natural antioxidant agents that can balance the antioxidant and ROS levels, resulting in the prevention of cell damage and degeneration of cellular contents.

Conclusion

Synthesis of metallic nanoparticles in a biological way had proven to be a method where the process is effective and less toxic. In the present study an endophytic fungus, *Talaromyces purpureogenus* was isolated from *Taxus baccata* Linn. The fungus showed its potency to reduce the AgNO_3 to AgNPs where it produced high-quality crystalline AgNPs and its characterization was done using various techniques viz. UV-vis spectroscopy, FTIR, FEG-SEM, HRTEM, and XRD. The functional groups found in FTIR analysis have a probable role as capping agents. The particles were found to have a size of about 49.3 nm with crystalline fcc nature. The AgNPs also showed their effect on both gram-positive and gram-negative bacteria. Thus, the results conclude that isolated fungus *Talaromyces*

purpureogenus is a distinguished producer of differently shaped silver nanoparticles having effective antibacterial and antioxidant activities, which can further accomplish biomedical and industrial purposes channelizing a way to reduce the pressure *Taxus baccata* is facing due to unethical harvesting techniques employed because of its huge utilitarian value.

Abbreviations

$^{\circ}\text{C}$: Degree Celsius; μL : Micro litre; μm : Micrometre; a.m.u: Atomic mass unit; Ag: Silver; AgNPs: AgNPs; cm: Centimetre; Da: Dalton; DLS: Dynamic light scattering; DMSO: Dimethyl sulfoxide; DPPH: 2,2'-Diphenyl-1-picrylhydrazyl; EDS: Energy dispersive X-ray diffraction; FCC: Face centered cubic; FEG-SEM: Field emission gun scanning electron microscopy; FTIR: Fourier transform infra red spectroscopy; g: Gram; GC-MS: Gas chromatography mass spectroscopy; h: Hour/hours; HCl: Hydrochloric acid; HRTEM: High resolution transmission electron microscopy; ICDD: International Centre of Diffraction Data; ITS: Internal transcribed spacers; JCPDS: Joint Committee on Power Diffraction Standards; L: Litre; Linn.: Linnaeus; MEEF: Mycelial extract of endophytic fungi; mg: Milligram; mg/L: Milligram/litre; MIC: Minimum inhibitory concentration; min: Minute; mL: Millilitre; mm: Millimetre; mM: Millimolar; mV: Millivolt; nm: Nanometre; PCR: Polymerase chain reaction; PDA: Potato dextrose agar; PDB: Potato dextrose broth; Pdl: Polydispersity index; r.nm: Radius in nanometre; rpm: Rotation per minute; sec: Second; UV-Vis: Ultra-violet visible spectroscopy; XRD: X-ray diffraction.

Acknowledgements

We would like to thank the Department of Biosciences, H.P.U. Shimla for the laboratory assistance. We would particularly thank CSIR-CSIO Chandigarh, PU-SAIF, and PU-CIL facility for different types of characterization. We would particularly like to thank Dr. S.K Singh, Scientist, National Facility (NFCCI and FIS) ARI, Pune; for molecular identification of fungal species. No funds or grants or other support was received.

Authors' contributions

All the authors read and approved the final manuscript.

Funding

No Funding/Grant was received for this research work.

Declarations

Competing interests

The authors declare that they have no competing interests.

Author details

¹Department of Biosciences, Himachal Pradesh University, Summerhill, Shimla 171005, Himachal Pradesh, India. ²Department of Genetics, Maharishi Dayanand University, Rohtak 124001, Haryana, India.

Received: 12 November 2021 Accepted: 8 January 2022

Published online: 20 January 2022

References

- Chaturvedi S, Dass S (2011) Traditional medicinal and economic uses of gymnosperms. *Bull Environ Pharmacol Life Sci* 1(1):70–72
- Cameron SJ, Smith RF (2002) Bringing “blue sky biology” down to earth: linking natural products research with commercialization. Proceedings of the 29th Annual Meeting of the Plant Growth Regulation Society of America, Halifax
- Beckstrom-Sternberg SM, Duke JA (1993) International Yew Resource Conference, Berkeley, p 3
- Mukherjee A, Joshi K, Pal RS, Atheequlla GA, Roy ML, Chandra N (2018) Scientific health benefits of namakeen chai/jya (salted tea): a traditional tea beverage of Bhotiya tribal community in higher altitudes of Uttarakhand. *Indian J Tradit Knowl* 17:365–369
- Gaur RD (1999) Flora of the district Garhwal, North West Himalaya. *Trans-media, Srinagar*
- Talebi M, Ghassempour A, Talebpour Z, Rassouli A, Dolatyari L (2004) Optimization of the extraction of paclitaxel from *Taxus baccata* L. by the use of microwave energy. *J Sep Sci* 27(13):1130–1136
- Malik S, Cusidó RM, Mirjalili MH, Moyano E, Palazón J, Bonfill M (2011) Production of the anticancer drug taxol in *Taxus baccata* suspension cultures: a review. *Process Biochem* 46(1):23–34
- Purohit A, Maikhuri RK, Rao KS, Nautiyal S (2001) Impact of bark removal on survival of *Taxus baccata* L. (Himalayan yew) in Nanda Devi biosphere reserve, Garhwal Himalaya, India. *Curr Sci* 81:586–590
- Nimasow G, Dai Nimasow O, Tsering G (2015) Vanishing *Taxus baccata* L. due to unsustainable exploitation and climate change in west Kameng and Tawang districts of Arunachal Pradesh. *Earth* 4(3–1):11–18
- Piovesan G, Saba EP, Biondi F, Alessandrini A, Di Filippo A, Schirone B (2009) Population ecology of yew (*Taxus baccata* L.) in the Central Apennines: spatial patterns and their relevance for conservation strategies. *Plant Ecol* 205(1):23–46
- Adhikari P, Pandey A (2020) Bioprospecting plant growth promoting endophytic bacteria isolated from Himalayan yew (*Taxus wallichiana* Zucc.). *Microbiol Res* 239:126536
- Ankush S, Anand S, Madhavi J (2017) Diversity of fungi associated with *Taxus baccata* Linn. in different seasons. *Indian For* 143(4):380–384
- Ashkezari SJ, Fotouhifar KB (2017) Diversity of endophytic fungi of common yew (*Taxus baccata* L.) in Iran. *Mycol Prog* 16(3):247–256
- Chaurasia B, Pandey A, Palni LMS (2005) Occurrence of arbuscular mycorrhizae in the rhizosphere of Himalayan Yew [*Taxus baccata* L. subsp. *wallichiana* (Zucc.) Pilger]—a case study. Basic research and applications of Mycorrhizae. IK International Pvt. Ltd., New Delhi, pp 26–35
- Yuan JI, Jian-Nan BI, Bing YAN, Xu-Dong Z (2006) Taxol-producing fungi: a new approach to industrial production of taxol. *Chin J Biotechnol* 22(1):1–6
- Wani ZA, Ashraf N, Mohiuddin T, Riyaz-Ul-Hassan S (2015) Plant-endophyte symbiosis, an ecological perspective. *Appl Microbiol Biotechnol* 99(7):2955–2965
- Li G, He D, Qian Y, Guan B, Gao S, Cui Y, Yokoyama K, Wang L (2012) Fungus-mediated green synthesis of silver nanoparticles using *Aspergillus terreus*. *Int J Mol Sci* 13(11):466–476
- Kajani AA, Bordbar AK, Esfahani SHZ, Khosropour AR, Razmjou A (2014) Green synthesis of anisotropic silver nanoparticles with potent anticancer activity using *Taxus baccata* extract. *RSC Adv* 4(106):61394–61403
- Kajani AA, Zarkesh-Esfahani SH, Bordbar AK, Khosropour AR, Razmjou A, Kardi M (2016) Anticancer effects of silver nanoparticles encapsulated by *Taxus baccata* extracts. *J Mol Liq* 223:549–556
- Sreekanth D, Syed A, Sarkar S, Sarkar D, Santhakumari B, Ahmad A, Khan MI (2009) Production, purification, and characterization of taxol and 10-DABIII from a new endophytic fungus *Gliocladium* sp. isolated from the Indian Yew Tree, *Taxus baccata*. *J Microbiol Biotechnol* 19(11):1342–1347
- Bhatnagar S, Kobori T, Ganesh D, Ogawa K, Aoyagi H (2019) Biosynthesis of silver nanoparticles mediated by extracellular pigment from *Talaromyces purpurogenus* and their biomedical applications. *Nanomaterials* 9(7):1042
- Hu X, Kandasamy Saravanakumar TJ, Wang MH (2019) Mycosynthesis, characterization, anticancer and antibacterial activity of silver nanoparticles from endophytic fungus *Talaromyces purpureogenus*. *Int J Nanomed* 14:3427
- Wang L, Wu Y, Xie J, Wu S, Wu Z (2018) Characterization, antioxidant and antimicrobial activities of green synthesized silver nanoparticles from *Psidium guajava* L. leaf aqueous extracts. *Mater Sci Eng C* 86:1–8
- Khan I, Saeed K, Khan I (2019) Nanoparticles: properties, applications and toxicities. *Arab J Chem* 12(7):908–931
- Shreyash N, Sonker M, Bajpai S, Tiwary SK (2021) Review of the mechanism of nanocarriers and technological developments in the field of nanoparticles for applications in cancer theragnostics. *ACS Appl Bio Mater* 4(3):2307–2334
- Mojab F, Kamalinejad M, Ghaderi N, Vahidipour HR (2010) Phytochemical screening of some species of Iranian plants. *Iran J Pharmaceut Res* 2:77–82
- Saravanakumar K, Sriram B, Sathiyaseelan A, Mariadoss AVA, Hu X, Han KS et al (2021) Synthesis, characterization, and cytotoxicity of starch-encapsulated biogenic silver nanoparticle and its improved anti-bacterial activity. *Int J Biol Macromol* 182:1409–1418
- Mukherjee P, Ahmad A, Mandal D, Senapati S, Sainkar SR, Khan MI et al (2001) Fungus-mediated synthesis of silver nanoparticles and their immobilization in the mycelial matrix: a novel biological approach to nanoparticle synthesis. *Nano Lett* 1(10):515–519
- Li WR, Xie XB, Shi QS, Zeng HY, You-Sheng OY, Chen YB (2010) Antibacterial activity and mechanism of silver nanoparticles on *Escherichia coli*. *Appl Microbiol Biotechnol* 85(4):1115–1122
- Chernousova S, Epple M (2013) Silver as antibacterial agent: ion, nanoparticle, and metal. *Angew Chem Int Ed* 52(6):1636–1653
- Gurunathan S, Park JH, Han JW, Kim JH (2015) Comparative assessment of the apoptotic potential of silver nanoparticles synthesized by *Bacillus tequilensis* and *Calocybe indica* in MDA-MB-231 human breast cancer cells: targeting p53 for anticancer therapy. *Int J Nanomed* 10:4203
- Bharde A, Rautaray D, Bansal V, Ahmad A, Sarkar I, Yusuf SM, Sanyal M, Sastry M (2006) Extracellular biosynthesis of magnetite using fungi. *Small* 2(1):135–141
- Bhainsa KC, D'souza SF (2006) Extracellular biosynthesis of silver nanoparticles using the fungus *Aspergillus fumigatus*. *Colloids Surf B* 47(2):160–164
- Mukherjee P, Roy M, Mandal BP, Dey GK, Mukherjee PK, Ghatak J, Tyagi AK, Kale SP (2008) Green synthesis of highly stabilized nanocrystalline silver particles by a non-pathogenic and agriculturally important fungus *T. asperellum*. *Nanotechnology* 19(7):075103
- Affify TA, Saleh HH, Ali ZI (2017) Structural and morphological study of gamma-irradiation synthesized silver nanoparticles. *Polym Compos* 38(12):2687–2694
- Shaheen MN, El-hadedy DE, Ali ZI (2019) Medical and microbial applications of controlled shape of silver nanoparticles prepared by ionizing radiation. *BioNanoScience* 9(2):414–422
- Govindappa M, Farheen H, Chandrappa CP, Rai RV, Raghavendra VB (2016) Mycosynthesis of silver nanoparticles using extract of endophytic fungi, *Penicillium* species of *Glycosmium mauritiana*, and its antioxidant, antimicrobial, anti-inflammatory and tyrosinase inhibitory activity. *Adv Nat Sci* 7(3):035014
- Farsi M, Farokhi S (2018) Biosynthesis of antibacterial silver nanoparticles by endophytic fungus *Nemania* sp. isolated from *Taxus baccata* L. (Iranian yew). *Zahedan J Res Med Sci*. <https://doi.org/10.5812/zjrms.57916>

39. Schulz B, Wanke U, Draeger S, Aust HJ (1993) Endophytes from herbaceous plants and shrubs: effectiveness of surface sterilization methods. *Mycol Res* 97(12):1447–1450
40. Suryanarayanan TS, Thennarasan S (2004) Temporal variation in endophyte assemblages of *Plumeria rubra* leaves. *Fungal Divers* 15:197–204
41. Saravanakumar K, Wang MH (2018) *Trichoderma* based synthesis of anti-pathogenic silver nanoparticles and their characterization, antioxidant and cytotoxicity properties. *Microb Pathog* 114:269–273
42. Saravanakumar K, Shanmugam S, Varukattu NB, MubarakAli D, Kathiresan K, Wang MH (2019) Biosynthesis and characterization of copper oxide nanoparticles from indigenous fungi and its effect of photothermolysis on human lung carcinoma. *J Photochem Photobiol B* 190:103–109
43. Radji M, Sumiati A, Rachmayani R, Elya B (2011) Isolation of fungal endophytes from *Garcinia mangostana* and their antibacterial activity. *Afr J Biotech* 10(1):103–107
44. Yadav M, Yadav A, Yadav JP (2014) In vitro antioxidant activity and total phenolic content of endophytic fungi isolated from *Eugenia jambolana* Lam. *Asian Pac J Trop Med* 7:S256–S261
45. Bhimba BV, Meenupriya J, Joel EL, Naveena DE, Kumar S, Thangaraj M (2010) Antibacterial activity and characterization of secondary metabolites isolated from mangrove plant *Avicennia officinalis*. *Asian Pac J Trop Med* 3(7):544–546
46. Devi NN, Shankar DP, Sutha S (2012) Biomimetic synthesis of silver nanoparticles from an endophytic fungus and their antimicrobial efficacy. *Int J Biomed Adv Res* 3:409–415
47. Rani R, Sharma D, Chaturvedi M, Yadav JP (2017) Green synthesis, characterization and antibacterial activity of silver nanoparticles of endophytic fungi *Aspergillus terreus*. *J Nanomed Nanotechnol*. <https://doi.org/10.4172/2157-7439.1000457>
48. Sandhu SS, Shukla H, Shukla S (2017) Biosynthesis of silver nanoparticles by endophytic fungi: its mechanism, characterization techniques and antimicrobial potential. *Afr J Biotech* 16(14):683–698
49. Brumfitt W, Hamilton-Miller JM, Franklin I (1990) Antibiotic activity of natural products: 1. Propolis. *Microbios* 62(250):19–22
50. Sarkar S, Jana AD, Samanta SK, Mostafa G (2007) Facile synthesis of silver nanoparticles with highly efficient anti-microbial property. *Polyhedron* 26(15):4419–4426
51. Blois MS (1958) Antioxidant determinations by the use of a stable free radical. *Nature* 181(4617):1199–1200
52. Oyaizu M (1986) Studies on products of browning reaction antioxidative activities of products of browning reaction prepared from glucosamine. *Jpn J Nutr Diet* 44(6):307–315
53. Awwad AM, Salem NM, Abdeen AO (2013) Green synthesis of silver nanoparticles using carob leaf extract and its antibacterial activity. *Int J Ind Chem* 4(1):1–6
54. Krishnaraj C, Jagan EG, Rajasekar S, Selvakumar P, Kalaichelvan PT, Mohan NJCSBB (2010) Synthesis of silver nanoparticles using *Acalypha indica* leaf extracts and its antibacterial activity against water borne pathogens. *Colloids Surf B* 76(1):50–56
55. Tyagi S, Tyagi PK, Gola D, Chauhan N, Bharti RK (2019) Extracellular synthesis of silver nanoparticles using entomopathogenic fungus: characterization and antibacterial potential. *SN Appl Sci* 1(12):1–9
56. Nair AS, Pradeep T (2003) Halocarbon mineralization and catalytic destruction by metal nanoparticles. *Curr Sci* 84:1560–1564
57. Sathiyaseelan A, Saravanakumar K, Mariadoss AVA, Wang MH (2020) Biocompatible fungal chitosan encapsulated phytochemical silver nanoparticles enhanced antidiabetic, antioxidant and antibacterial activity. *Int J Biol Macromol* 153:63–71
58. Devi LS, Joshi SR (2015) Ultrastructures of silver nanoparticles biosynthesized using endophytic fungi. *J Microsc Ultrastruct* 3(1):29–37
59. Jyoti K, Baunthiyal M, Singh A (2016) Characterization of silver nanoparticles synthesized using *Urtica dioica* Linn. leaves and their synergistic effects with antibiotics. *J Radiat Res Appl Sci* 9(3):217–227
60. Madakka M, Jayaraju N, Rajesh N (2018) Mycosynthesis of silver nanoparticles and their characterization. *MethodsX* 5:20–29
61. Yazdi MET, Khara J, Housaindokht MR, Sadeghnia HR, Bahabadi SE, Amiri MS, Mosawee H, Taherzadeh D, Darroudi M (2019) Role of *Ribes khorasanicum* in the biosynthesis of AgNPs and their antibacterial properties. *IET Nanobiotechnol* 13(2):189–192
62. Prakash P, Gnanaprakasam P, Emmanuel R, Arokiyaraj S, Saravanan M (2013) Green synthesis of silver nanoparticles from leaf extract of *Mimusops elengi* Linn. for enhanced antibacterial activity against multi drug resistant clinical isolates. *Colloids Surf B* 108:255–259
63. Manikprabhu D, Lingappa K (2013) Microwave assisted rapid and green synthesis of silver nanoparticles using a pigment produced by *Streptomyces coelicolor* klmp33. *Bioinorg Chem Appl*. <https://doi.org/10.1155/2013/341798>
64. Aravinthan A, Govarthanan M, Selvam K, Praburaman L, Selvakumar T, Balamurugan R, Kamala-Kannan S, Kim JH (2015) Sunroot mediated synthesis and characterization of silver nanoparticles and evaluation of its antibacterial and rat splenocyte cytotoxic effects. *Int J Nanomed* 10:1977
65. Singh T, Jyoti K, Patnaik A, Singh A, Chauhan R, Chandel SS (2017) Biosynthesis, characterization and antibacterial activity of silver nanoparticles using an endophytic fungal supernatant of *Raphanus sativus*. *J Genet Eng Biotechnol* 15(1):31–39
66. Roy S, Mukherjee T, Chakraborty S, das Kumar T (2013) Biosynthesis, characterisation and antifungal activity of silver nanoparticles by the fungus *Aspergillus foetidus* MTCC8876. *Digest J NanomaterBiostruct* 8:197–205
67. Shaligram NS, Bule M, Bhambure R, Singhal RS, Singh SK, Szakacs G, Pandey A (2009) Biosynthesis of silver nanoparticles using aqueous extract from the compactin producing fungal strain. *Process Biochem* 44(8):939–943
68. Suresh AK, Doktycz MJ, Wang W, Moon JW, Gu B, Meyer HM III et al (2011) Monodispersed biocompatible silver sulfide nanoparticles: facile extracellular biosynthesis using the γ -proteobacterium *Shewanella oneidensis*. *Acta Biomater* 7(12):4253–4258
69. Kotakadi VS, Gaddam SA, Venkata SK, Sarma PVGK, Sai Gopal DVR (2016) Biofabrication and spectral characterization of silver nanoparticles and their cytotoxic studies on human CD34 +ve stem cells. *Biotech* 6(2):216
70. Balaji DS, Basavaraja S, Deshpande R, Mahesh DB, Prabhakar BK, Venkataraman A (2009) Extracellular biosynthesis of functionalized silver nanoparticles by strains of *Cladosporium cladosporioides* fungus. *Colloids Surf B* 68(1):88–92
71. Chen JC, Lin ZH, Ma XX (2003) Evidence of the production of silver nanoparticles via pretreatment of *Phoma* sp. 3.2883 with silver nitrate. *Lett Appl Microbiol* 37(2):105–108
72. Okafor F, Janen A, Kukhtareva T, Edwards V, Curley M (2013) Green synthesis of silver nanoparticles, their characterization, application and antibacterial activity. *Int J Environ Res Public Health* 10(10):5221–5238
73. Lee W, Kim KJ, Lee DG (2014) A novel mechanism for the antibacterial effect of silver nanoparticles on *Escherichia coli*. *Biometals* 27(6):1191–1201
74. Nurul Aini A, Al Farraj DA, Endarko E, Rubiyanto A, Nur H, Al Khulaifi MM, Hadibarata T, Syafuddin A (2019) A new green method for the synthesis of silver nanoparticles and their antibacterial activities against gram-positive and gram-negative bacteria. *J Chin Chem Soc* 66(7):705–712

Publisher's Note

Springer Nature remains neutral with regard to jurisdictional claims in published maps and institutional affiliations.

Submit your manuscript to a SpringerOpen® journal and benefit from:

- Convenient online submission
- Rigorous peer review
- Open access: articles freely available online
- High visibility within the field
- Retaining the copyright to your article

Submit your next manuscript at ► [springeropen.com](https://www.springeropen.com)